PHYSICAL REVIEW B **74**, 115321 (2006)

Quantum gate based on Stark tunable nanocrystal interactions with ultrahigh-Q/V field modes in fused silica microcavities

Mark J. Fernée and Halina Rubinsztein-Dunlop
Center for Quantum Computer Technology, The University of Queensland, Queensland 4072, Australia
(Received 23 January 2006; revised manuscript received 21 June 2006; published 22 September 2006)

We investigate the use of nanocrystal quantum dots as a quantum bus element for preparing various quantum resources for use in photonic quantum technologies. Using the Stark-tuning property of nanocrystal quantum dots as well as the biexciton transition, we demonstrate a photonic controlled-NOT (CNOT) interaction between two logical photonic qubits comprising two cavity field modes each. We find the CNOT interaction to be a robust generator of photonic Bell states, even with relatively large biexciton losses. These results are discussed in light of the current state of the art of both microcavity fabrication and recent advances in nanocrystal quantum dot technology. Overall, we find that such a scheme should be feasible in the near future with appropriate refinements to both nanocrystal fabrication technology and microcavity design. Such a gate could serve as an active element in photonic-based quantum technologies.

DOI: 10.1103/PhysRevB.74.115321 PACS number(s): 78.67.Bf, 42.50.Dv, 42.50.Ct

INTRODUCTION

All-optical quantum computing is an area of current interest due to the fact that the quantum information carried by photons is extremely robust. This property stems from the fact that photons interact weakly with the environment. A corollary of this is that photons only weakly interact with each other. Thus, it was thought that conditional gate operations with photons would prove to be practically impossible. Surprisingly, Knill *et al.*[1] discovered that nondeterministic quantum gate operations were actually possible using only simple linear optical elements. Furthermore they showed that it could be possible to build a scalable quantum computer using their architecture. Recent experiments have already demonstrated the basic building blocks for all-optical quantum computing.[2–4]

While all-optical quantum computing has made considerable progress both theoretically and experimentally, it has a number of major hurdles that still must be overcome. The nondeterministic gate operation means that useful quantum circuits suffer dreadful scaling problems, the optical circuitry is still rather large and cumbersome, and compact and reliable single-photon sources are required.

Many of the hurdles associated with all-optical quantum computing could be overcome if the circuitry required to compensate for the nondeterministic nature of the gates could be replaced by a simple deterministic nonlinear gate element.[5] Such a gate element would dramatically reduce the overhead required by all-optical quantum computing and potentially allow for miniaturization of the optical quantum circuits.

A suitable nonlinear gate element could be realized using cavity quantum electrodynamics (CQED) in the strong-coupling regime to enhance the nonlinear interaction between a single photon and a single quantum object such as an atom. Many possible quantum gates have already been demonstrated in the microwave regime and proposed for the optical regime. Furthermore, miniaturization of CQED schemes has progressed steadily over the last few years. The development of high-quality silica microtori[6,7] and photonic band-gap structures[8] means that some of the basic building blocks are already in place for producing miniature quantum gates. In particular, miniature fused silica microcavities have already been identified as the most promising candidates for cavity QED in the optical regime.[6,7,9,10]

However, if we are to pursue miniature quantum gates based on CQED, we need a suitable quantum object. The use of atoms or ions would be ideal if it were possible to trap a single atom or ion and place it into the cavity field. This has already been demonstrated for neutral atoms,[11] but is in practice an extremely difficult task, the main difficulty being that optically active atoms and ions are also extremely chemically active and so have to be carefully isolated from their surroundings.

Alternatively, nanocrystal quantum dots are often referred to as "artificial atoms" and so should also be considered as a suitable quantum object. One main advantage is that while quantum dots are optically active, the ideal quantum dot is not chemically active. Therefore, quantum dots can be incorporated into CQED systems without the need for strong chemical isolation. Furthermore, the position of a quantum dot relative to the cavity field can remain fixed, thus dramatically simplifying the CQED interaction dynamics. Nanocrystal quantum dots coupled to microcavities have already been used to demonstrate single-photon sources.[12–15] Quantum gates based on cavity-enhanced interactions between quantum dots have been proposed[16] and a quantum gate based on the states within a single quantum dot has already been demonstrated.[17] Therefore it seems that the use of a quantum dot as a quantum object for use in a CQED-based quantum gate is worth considering.

There are two distinct types of nanocrystal quantum dot: The isolated nanocrystal grown using colloidal chemistry[18–20] and the epitaxially grown nanocrystal island embedded within a semiconductor substrate[12,17,21–23] [often referred to as a self-assembled quantum dot (SAQD)]. While the technology and understanding of nanocrystals has progressed dramatically over the last 15 years, there remain substantial differences between the physical properties of these two types of nanocrystal. Epitaxial quantum dots come clos-

est to the ideal quantum dot in that the epitaxial continuation of the crystal structure prevents charge carrier trapping at the quantum dot surface. Therefore, charge carriers in these quantum dots are either unbound above the confinement potential, or exist in a finite number of discrete bound states below the confinement potential. Epitaxially grown nanocrystals have already proven useful in various quantum technologies, including cavity-enhanced single-photon sources.[12–15] Vacuum Rabi splitting has also been reported for cavity-coupled quantum dots.[22,23] Quantum gate operation has also been demonstrated by manipulating the intrinsic states of a single epitaxially grown quantum dot.[17]

Colloidal quantum dots offer some key advantages such as not being attached to a substrate as well as size and shape tunability. These properties should make them extremely useful for use in hybrid optical-semiconductor schemes, such as CQED with silica microresonators, where a colloidal nanocrystal can be placed at an arbitrary point within the cavity field[24–26] and possibly even in an arbitrary orientation. Nevertheless, there are many technical difficulties that still remain to be overcome. For instance, colloidal nanocrystals are known to blink[27–29] and undergo spectral diffusion.[30,31] These two properties are thought to be related to the presence of, and accessibility to, charge trapping sites just outside the quantum dot. For blinking, either direct trapping of a single intrinsic charge carrier or ejection of a charge carrier due to the process of Auger ionization is thought to be the primary cause.[32] Spectral diffusion is due to the sensitivity of the quantum dot excited-state dipole to an external field, so that randomly trapped charges can cause fluctuations of the excited-state energy. In both cases, these unwanted processes are due to the close proximity of charge trapping sites to the intrinsic charge carriers within the quantum dot. In contrast, the process of making epitaxial SAQD's naturally minimizes charge-trapping defects near the quantum dot, although these are not necessarily eliminated altogether.[13] Nevertheless, cavity-coupled colloidal CdSe quantum dots have already been shown to exhibit Purcell enhancement of the spontaneous emission[24,25] as well as evidence of vacuum Rabi splitting.[26]

In this paper we investigate the use of colloidal nanocrystals in CQED-based quantum circuits drawing known properties from the state of the art in colloidal nanocrystal research as well as high-Q microcavity research. We propose an optical controlled-NOT (CNOT) gate using a single colloidal quantum dot as a quantum bus. By tuning the quantum dot resonance using dc Stark shifting, we show that there is a possibility of addressing multiple cavity modes with a single quantum dot, enabling high-speed gate operations to be conducted. All operations needed for the gate are modeled using master equation techniques to ensure that system losses are carefully accounted for. We discuss the results in light of the known properties of the various physical elements.

GATE OPERATION PRINCIPLE

One of the earliest demonstrations of quantum gate operation was reported by Haroche and co-workers using Rydberg atoms traveling through superconducting niobium microwave cavities.[33] The most well known of these schemes involved the use of a three-level atom comprising two successive Rydberg transitions. This gate was very well suited to microwave CQED as the two transition frequencies are very close to each other. An analogous three-level scheme is also possible using transitions in quantum dots. If one considers both the exciton and biexciton transitions, a very similar three-level system is possible. Recent reports of highly efficient biexciton recombination[34,35] and efficient charge multiplication[36] suggest that the biexciton may indeed be useful in quantum technologies. In fact, it is the larger nanocrystal quantum dots that provide the greatest promise, as only a modest degree of quantum confinement is required to provide an isolated transition, and larger nanocrystals exhibit dramatically reduced Auger ionization, which is the dominant multiexciton loss mechanism.[32]

Here we investigate the use of the biexciton to provide a conditional phase shift by using Stark tuning to bring the biexcitonic transition into resonance with a microcavity field mode. In this case, it is useful that the biexcitonic shift is small, so that both the exciton and biexciton resonance can be Stark tuned to the same cavity mode, which is necessary for both state preparation and gate operation. The biexciton shift in CdSe nanocrystals is of the order of 10 meV, which is well within the 35 meV Stark tunable range of a CdSe nanocrystal that has been previously reported.[40] The implementation of a CNOT gate based on a three-level "atom" means that the entire gate sequence can be accomplished rapidly using Stark shifting pulses and vacuum Rabi cycling. For a lifetime-limited excitonic transition in a CdSe nanocrystal, the ratio of the coupling frequency to the loss rate can be of the order of 100. Therefore, vacuum Rabi cycling should be possible with minimal loss. While this regime has yet to be demonstrated with any cavity QED interaction at optical frequencies, a similar operating regime has been predicted for atoms interacting with the field modes of various fused silica microcavities.[7,10]

The exact form of the microcavity may range from microspheres to microtoroids, the important factor being the presence of sufficient high-Q cavity modes in a reasonably small spectral range. We will return to this requirement later, but for now assume that nanocrystal can be brought into resonance with at least four high-Q field modes using the dc Stark effect.[40]

In contrast to the gate demonstrated in microwave cavity QED,[33] the "atom" in our gate travels through frequency space, and thus can remain fixed in real space. The proposed physical gate is depicted in Fig. 1(a), consisting of a single nanocrystal quantum dot placed on the surface of a high-Q/V fused silica microcavity (a toroidal cavity is depicted) with a fiber taper to couple out the cavity modes to a detector. Electrodes are placed nearby to allow Stark tuning of the nanocrystal resonance and a laser is used to excite the nanocrystal in order to initialize the states of the system. The biexciton transition is used to implement a conditional phase gate that forms the basis of the CNOT gate, is illustrated in Fig. 1(b). The quantum state can be a superposition between the ground and the single-exciton state $|X\rangle$, which is depicted in the diagram by thick lines. Only the single-exciton state undergoes the phase shift if there is a photon in the control

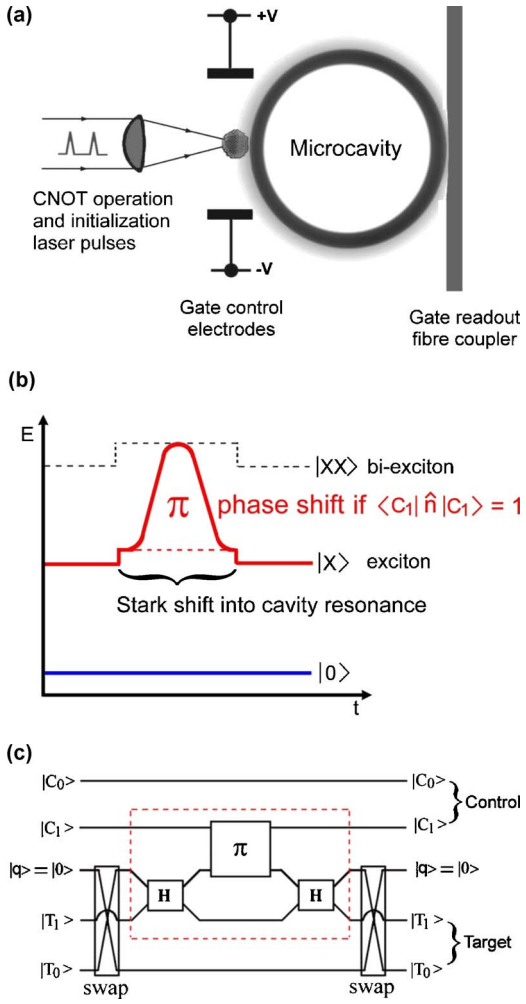

FIG. 1. (Color online) (a) Schematic of a proposed experimental implementation. A single nanocrystal quantum dot on the surface of a toroidal microcavity. Laser pulses are used for both initial-state preparation and the CNOT operation. Electrodes are used for Stark tuning the quantum dot between the different cavity resonances. A fiber taper is used to couple the field modes to the detection system. (b) The three levels of the quantum dot system. Both the ground state $|0\rangle$ and the exciton state $|X\rangle$ can be occupied in any superposition state and so are illustrated using thick colored lines. The biexciton state $|XX\rangle$ does not contain any quantum information, so is unoccupied during most of the gate operation and is represented by a dashed line. The Stark tuning of the biexciton transition into resonance with the control qubit $|1\rangle$ state cavity mode is illustrated. Transient occupation of the biexciton level is possible only if there is a photon in the cavity mode. (c) A diagram representing all relevant quantum objects involved in the photonic CNOT gate. Four field modes, comprising the two logical qubits as well as the quantum dot state, are indicated. Only single-photon occupancy is permitted in the computational basis. The quantum dot acts solely as a quantum bus. Therefore the first operation is a swap gate that loads the information in the target qubit $|0\rangle$ state into the quantum dot. A Hadamard gate is then implemented between the quantum dot and the target qubit $|1\rangle$ state. The quantum dot then undergoes a conditional phase shift and the sequence is reversed, leaving all the quantum information in the photonic qubits and the quantum dot in the ground state. The dashed box includes the part of the photonic CNOT gate that is simulated. The swap gates are simulated separately.

mode resonant with the biexciton transition. The biexciton state $|XX\rangle$ is indicated by a dashed line in order to show that it is only transiently populated during the gate operation. This mode of operation does require the splitting of the spin degeneracy of the exciton state. This can be accomplished with an applied magnetic field.[41]

The all-optical or photonic CNOT gate thus uses the field-atom conditional phase shift interaction. However, both prior to and immediately following the phase gate interaction, the quantum information is stored solely in the optical field modes. Thus the atom (quantum dot) is used to read and manipulate the quantum information contained in the field modes. A schematic for a four-mode all-optical CNOT gate is presented in Fig. 1(c). Here the quantum information is represented in a logical qubit basis comprising two field modes to represent a single qubit. Therefore, a requirement of the quantum dot is that the excitonic resonance can be Stark tuned across all four cavity modes, while the biexcitonic resonance can be tuned into resonance with the field mode representing the control qubit in the $|1\rangle$ state. Such a logical qubit system has the advantage that atomic losses result in states that exist outside the computational basis and hence are easily detected. This is especially useful for detecting Auger ionization losses from the biexciton state.[32]

Following Fig. 1(c) and assuming prior state initialization, the CNOT gate operation proceeds as follows. The quantum dot is Stark tuned into resonance with the target $|0\rangle$ state and the state swapped by waiting half a Rabi period (π rotation). The quantum dot is then Stark tuned into resonance with the target $|1\rangle$ state and mixed by waiting a quarter of a Rabi cycle ($\pi/2$ rotation, or Hadamard gate). The quantum dot is then Stark tuned to a point where the biexciton transition is resonant with the control $|1\rangle$ state to achieve a conditional π phase shift by waiting for a time sufficient for a 2π Rabi cycle of the biexciton resonance. The state of the quantum dot is then returned to the target field modes via the reverse process of a Hadamard gate with the target $|1\rangle$ state and then a swap gate with the target $|0\rangle$ state using the appropriate Stark tuning pulses.

The use of a logical computational basis has many benefits for experimental implementation. The use of two field modes per qubit means that arbitrary superposition states can be prepared from a single quantum dot excitation, by a process of vacuum Rabi cycling that transfers a fraction of the excitation to one mode and the remainder to the other. This allows a quantum state to be rapidly prepared in a time far shorter than the lifetime of the quantum dot excited state. Two successive excitations of the quantum dot can therefore be used to rapidly prepare the initial two-qubit quantum state of the CNOT system. The other major benefit is that the use of a logical basis can ensure that certain system losses are readily detected and can be corrected by rerunning the gate. Therefore, the statistics of gate operation can be obtained only from operations where two quanta are detected in the appropriate modes. These types of quantum schemes form excellent test beds for quantum gates, as they allow for the use of inefficient detection systems.[2]

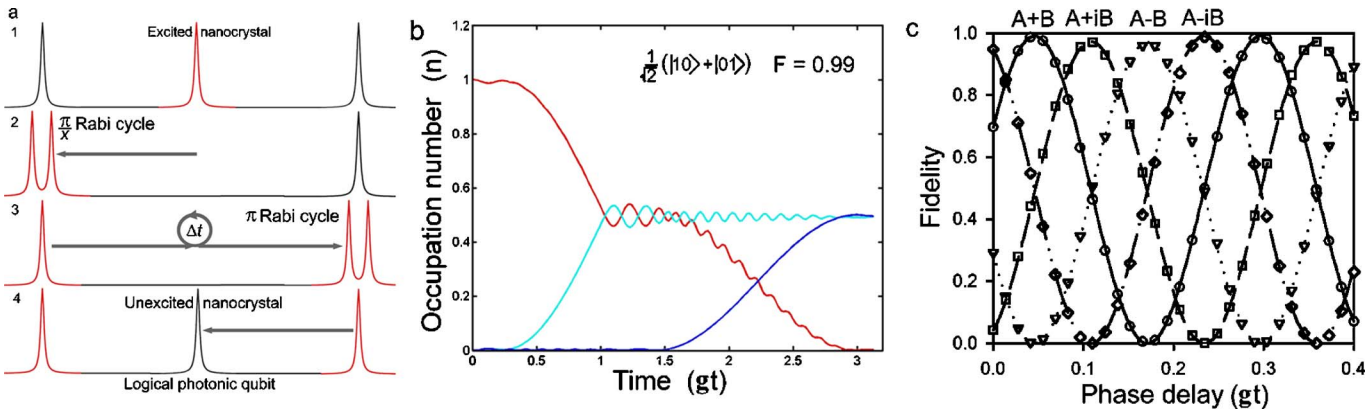

FIG. 2. (Color online) (a) An illustration of the logical qubit initialization sequence. The peaks represent two field modes of the microcavity system (on each end) and the nanocrystal resonance (in the center). Step 1: the nanocrystal is promoted to its excited state. Step 2: the nanocrystal is rapidly Stark tuned on to resonance with the left cavity mode for a time corresponding to a predetermined fraction of a Rabi cycle. Step 3: the nanocrystal is rapidly Stark tuned on to resonance with the right cavity mode. A certain delay Δt is introduced to adjust the phase of the qubit. The nanocrystal is left on resonance for a time sufficient to accomplish a π Rabi cycle. Step 4: the now unexcited nanocrystal is rapidly Stark tuned away from the cavity mode resonances, leaving the two cavity modes in a known superposition state of zero and one photon (a logical qubit). (b) The simulated output for the logical qubit initialization sequence (including the maximum fidelity that can be achieved for creating the symmetric superposition state). The quantum dot state is easily identified as it starts in the excited state (unity occupation probability) and at the end of the sequence the quantum dot is returned to the ground state (zero occupation probability). (c) The fidelity plotted as a function of the delay time for creating either of four superposition states that vary only in their phase (by steps of $\pi/2$), indicating that any point on the Bloch sphere can be reached.

INITIAL-STATE PREPARATION

The most direct means of preparing an initial photonic qubit in the logical basis is by first exciting the nanocrystal in order to produce an electron-hole pair (i.e., an exciton, which recombines with the emission of a photon). Excitation of the nanocrystal may be done in a number of ways, the most direct being via optical absorption. The initialization sequence, illustrated in Fig. 2(a), proceeds as follows. The excited nanocrystal is rapidly Stark tuned into resonance with the first cavity mode, representing either the logical $|0\rangle$ or logical $|1\rangle$ state and is left to Rabi cycle for some predetermined time. The Rabi cycling is ended, by rapidly tuning the nanocrystal out of resonance, when the required probability amplitude for the state is reached. The nanocrystal is then Stark tuned into resonance with the second mode comprising the logical qubit and is left to Rabi cycle for exactly half a cycle, so that the remainder of the probability amplitude is transferred into the field mode. This also leaves the nanocrystal in the unexcited state, allowing it to be used either to prepare another logical qubit or in the CNOT gate. Phase rotations around the Bloch sphere are achieved by adjusting the time Δt between the two Rabi interactions.

A simulation of the preparation of the symmetric superposition state $\sqrt{\frac{1}{2}}(|10\rangle+|01\rangle)$ is shown in Fig. 2(b), which can be accomplished with a fidelity of 0.99. [Note: the fidelity used here is defined as $\mathrm{Tr}(\hat{\rho}_{out}\hat{\rho}_{sim})$, where $\hat{\rho}_{out}$ is the desired output state and $\hat{\rho}_{sim}$ is the simulated output.] The timing delay required to adjust the phase of the superposition is shown in Fig. 2(c). Here we have plotted the fidelities of obtaining either the symmetric, antisymmetric, or the two quadrature superposition states. The oscillations provide an indication that the phase of the state is uniformly rotating around the Bloch sphere. These simulations indicate that arbitrary initial states in a logical qubit basis can be created with high fidelity from a single nanocrystal excitation.

SIMULATION OF THE CNOT INTERACTION

Simulations of the field-atom system were carried out using two field modes and a three-level atomic system, comprising the subsystem indicated in the dashed box in Fig. 1(c). One of the field modes represents the control qubit in the state $|1\rangle$, while the other field mode represents the target qubit in the state $|1\rangle$. The remainder of the target qubit (i.e., the amplitude of the target state $|0\rangle$) is assumed to be already transferred to the quantum dot exciton state. The Hamiltonian for the three-level system interacting with two spectrally separated cavity field modes is represented in its general form as follows:

$$\hat{H}/\hbar = \sum_{i=C,T} \omega_i \hat{a}_i^\dagger \hat{a}_i + \sum_{j=1}^{3} [\omega_j + A_j(t)]|j\rangle\langle j| + \sum_{i=C,T} \sum_{j=1}^{2} i g_j (\hat{a}_i |j+1\rangle\langle j| - \text{h.c.}), \quad (1)$$

where $\hat{a}_C$ and $\hat{a}_T$ are the annihilation operators for the control and target qubit field modes which have frequencies ω_C and ω_T. The atomic operators are expressed in terms of projection operators with the energies of the three levels given by ω_j for $j=1,2,3$. The field-atom coupling strengths are represented by the parameters g_j for $j=1,2$. This Hamiltonian has a single time-dependent term $A(t)$, which represents the time-dependent Stark shifting pulse sequence that is used to operate the CNOT gate.

For the simulation we operate in a frame rotating at the control qubit frequency and terms far from resonance have

been neglected.[37] We rewrite the generalized three-level system in terms of exciton and biexciton operators $\hat{\sigma}_-^X = |1\rangle\langle 2|$ and $\hat{\sigma}_-^{XX} = |2\rangle\langle 3|$ and the associated detunings from the control qubit frequency. The Hamiltonian is thus recast into the following form:

$$\hat{H}/\hbar = \Delta_m \hat{a}_T^\dagger \hat{a}_T + \Delta_X \hat{\sigma}_+^X \hat{\sigma}_-^X + (\Delta_{XX} + \Delta_X)\hat{\sigma}_+^{XX}\hat{\sigma}_-^{XX} + ig_X \sum_{i=C,T} (\hat{a}_i \hat{\sigma}_+^X - \hat{a}_i^\dagger \hat{\sigma}_-^X) + ig_{XX} \sum_{i=C,T} (\hat{a}_i \hat{\sigma}_+^{XX} - \hat{a}_i^\dagger \hat{\sigma}_-^{XX}) + A(t)(\hat{\sigma}_+^X \hat{\sigma}_-^X + \hat{\sigma}_+^{XX}\hat{\sigma}_-^{XX}). \quad (2)$$

The constant $\Delta_m = \omega_T - \omega_C$ corresponds to separation between the cavity modes, while $\Delta_X = \omega_2 - \omega_1 - \omega_C$ and $\Delta_{XX} = \omega_3 - \omega_2 - \omega_C$ correspond to the frequency detunings of the quantum dot excitonic and biexcitonic transitions, respectively, from the control qubit frequency. The exciton and biexciton coupling frequencies g_1 and g_2 are now labeled g_X and g_{XX}. The time-dependent Stark shifting term $A(t)$ represents a sequence of Stark shifting pulses. The first pulse is used to perform a Hadamard gate between the quantum dot exciton state and the target qubit cavity mode. The quantum dot is then Stark tuned so that the biexciton transition is resonant with the control qubit field mode for a time sufficient to cause a complete Rabi cycle and a π phase shift. The quantum dot is then Stark tuned back into resonance with the target qubit cavity mode where another Hadamard gate is performed between the quantum dot exciton state and the target qubit cavity mode. This subset of the entire gate operation sequence was chosen in order to minimize the effective Hilbert space required for the simulation. The extra swap gates that are used in the entire gate sequence have been simulated separately.

In order to simulate actual gate operation, we include loss terms using the master equation in standard Linblad form. In this case, the master equation is simply represented as follows:

$$L = \frac{1}{i}[\hat{H}, \hat{\rho}] + \sum_{l=1}^{4} [\hat{C}_l \hat{\rho} \hat{C}_l^\dagger - \frac{1}{2}(\hat{C}_l^\dagger \hat{C}_l \hat{\rho} + \hat{\rho}\hat{C}_l^\dagger \hat{C}_l)] \quad (3)$$

where $\hat{H}$ is the Hamiltonian described above and $\hat{\rho}$ is the reduced density operator. The loss terms $\hat{C}_1 = \sqrt{\kappa}\hat{a}_T$, $\hat{C}_2 = \sqrt{\kappa}\hat{a}_C$, $\hat{C}_3 = \sqrt{\gamma_X}\hat{\sigma}_-^X$, and $\hat{C}_4 = \sqrt{\gamma_{XX}}\hat{\sigma}_-^{XX}$ represent the coupling of both the target and control cavity modes to other modes outside the cavity, and the spontaneous emission from both the exciton and biexciton states, respectively, with γ_X and γ_{XX} being the spontaneous emission decay rates of the exciton and biexciton states and κ is the cavity decay rate for both field modes.

We numerically integrate the master equation in order to simulate the gate operation. Using the Stark pulse sequence illustrated in Fig. 3, we simulate all the states represented in the CNOT truth table. The results presented in Fig. 4 represent the populations of the two field modes and the atom during the course of the interaction. The fidelity of the gate operation is also included. These simulations represent the case where the spontaneous emission loss of the biexciton state is equal to that of the exciton state, with $\gamma_X/g_X = \gamma_{XX}/g_{XX} = 0.01$. This is the low-loss case and is simply used to illustrate the CNOT interaction. We have also run the simulation for a range of γ_{XX}/g_{XX} values and the resulting fidelities for all operations comprising the CNOT truth table are given in Table I.

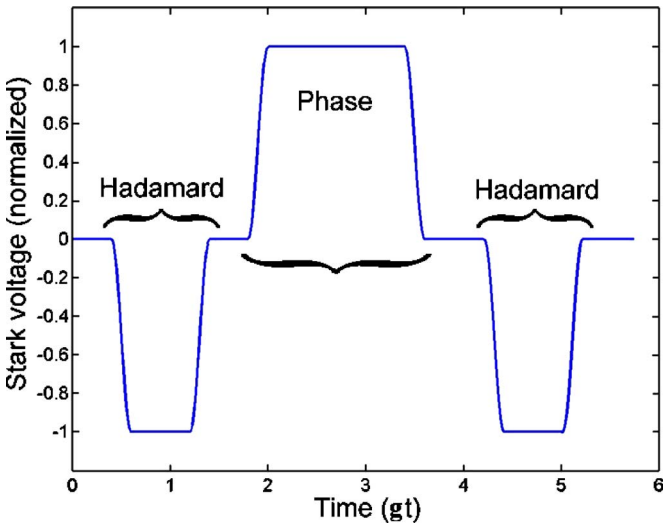

FIG. 3. (Color online) The Stark shift pulse sequence used to implement a CNOT interaction between two field modes. The initial and final Hadamard pulses are used to Stark shift the exciton state into resonance with the target $|1\rangle$ state to initiate Rabi cycling between the nanocrystal and cavity mode. A $\pi/2$ Rabi cycle is applied in each case. The phase gate is implemented by Stark shifting the biexciton transition into resonance with the control quibit $|1\rangle$ state. A 2π Rabi cycle is applied in order to generate a π phase shift of the exciton state $|X\rangle$.

The ultimate test of the CNOT interaction is its ability to generate entangled or Bell states. The fidelities of Bell state formation are included in Table II below, for the same range of γ_{XX}/g_{XX} values used in Table I.

READOUT

The proposed gate relies on coupling to an output fiber in order to transfer cavity photons to freely propagating fiber modes. The output photons must then be spectrally discriminated into four detector channels, two for each qubit. This spectral discrimination will require the use of narrowband filters with a bandwidth selectivity of between 1 and 10 GHz. Such selectivity can be achieved using interference techniques, such as tunable Fabry-Pérot étalons, which are more than capable of providing the necessary resolution and selectivity.[38] An even more promising and flexible scheme can be implemented using acousto-optic modulators.[39] Such technology is already in wide use for wavelength division multiplexing and so presents no technological barrier. The detection apparatus will then determine if a proper gate operation was accomplished using a coincidence logic scheme that will register a (potentially) successful gate operation only if two photons are detected, with one in either of the logical control modes and one in either of the logical target

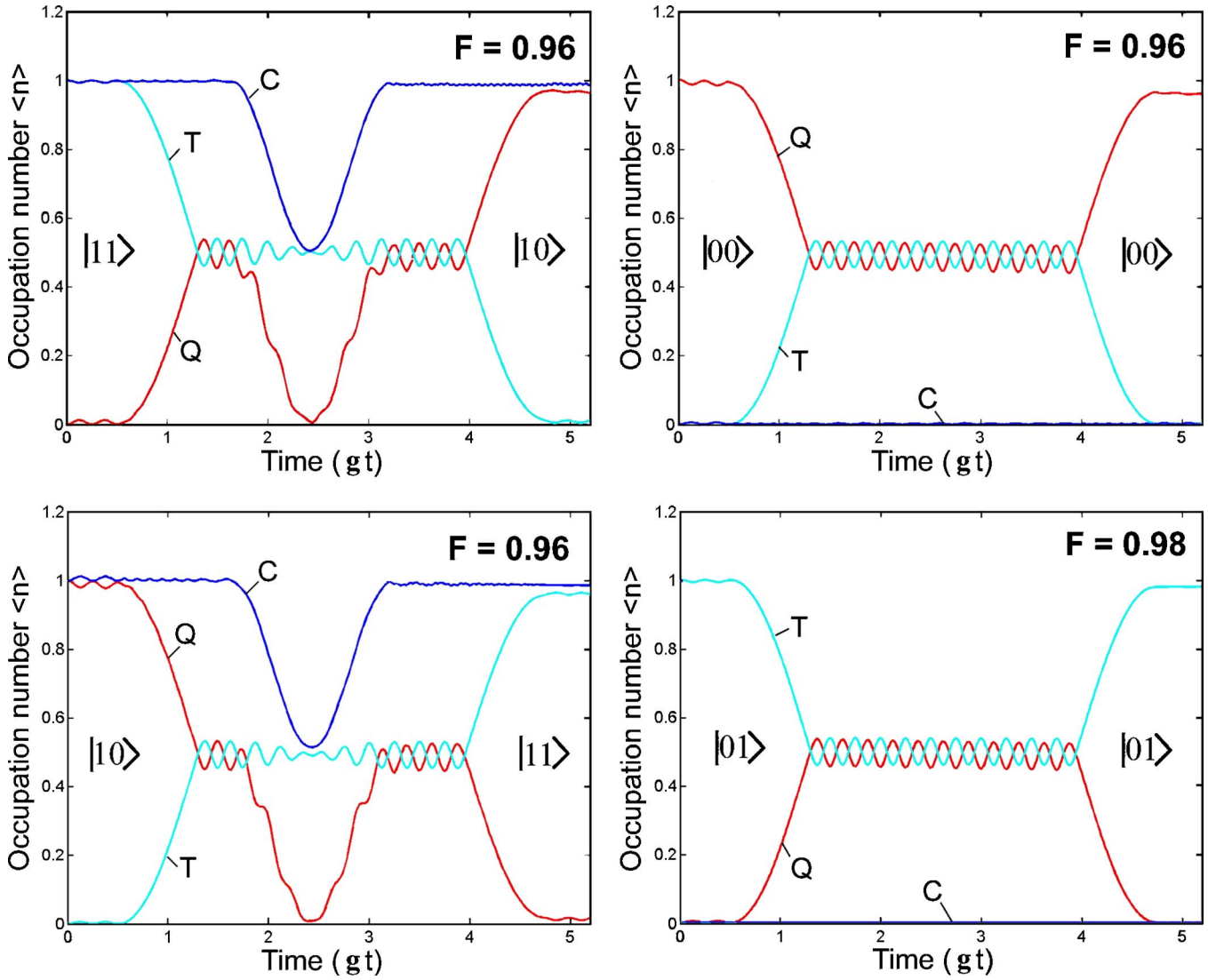

FIG. 4. (Color online) A series of simulated CNOT interactions for the biexcitonic gate representing the CNOT truth table. State occupation probabilities for the control $|1\rangle$ state (C) and the target $|1\rangle$ state (T) and the quantum dot (Q) are indicated. The occupation number of the quantum dot represents the population in the exciton state $|X\rangle$. Input and output states are indicated and the gate fidelity is also given. $g_X/\gamma_X = g_{XX}/\gamma_{XX} = 100$ and $g_X/\kappa = 1000$ are used for these simulations in order to demonstrate the basic CNOT interaction.

modes. This readout scheme thus also performs some simple error detection, which will increase the effective fidelities, conditioned on the appropriate combination of two photons being detected. Therefore it is not necessary to include the efficiencies in the detection apparatus, as these will invariably result in photon loss, which is detected. The proposed readout scheme is depicted in Fig. 5, including photon loss detecting logic.

STARK TUNING THE NANOCRYSTAL

The central idea in our proposed gate is to tune the nanocrystal excited-state energy using the dc Stark effect. This can allow frequency tuning across a wide spectral range, depending on the polarizability of the excitonic state. The polarizability of many of the available nanocrystals is not well known. However, most nanocrystal quantum dots dis-

TABLE I. Fidelity for CNOT operation.

CNOT operation	0.01	0.1	0.2	0.5	1
$\|11\rangle \rightarrow \|10\rangle$	0.96	0.92	0.89	0.80	0.67
$\|10\rangle \rightarrow \|11\rangle$	0.96	0.93	0.89	0.80	0.67
$\|01\rangle \rightarrow \|01\rangle$	0.98	0.98	0.98	0.98	0.98
$\|00\rangle \rightarrow \|00\rangle$	0.96	0.96	0.96	0.96	0.96

TABLE II. Fidelity for generation of Bell states.

Bell state	0.01	0.1	0.2	0.5	1
$\|10\rangle + \|01\rangle$	0.96	0.95	0.94	0.90	0.85
$\|10\rangle - \|01\rangle$	0.96	0.95	0.94	0.90	0.85
$\|11\rangle + \|00\rangle$	0.96	0.94	0.93	0.89	0.84
$\|11\rangle - \|00\rangle$	0.96	0.94	0.93	0.89	0.84

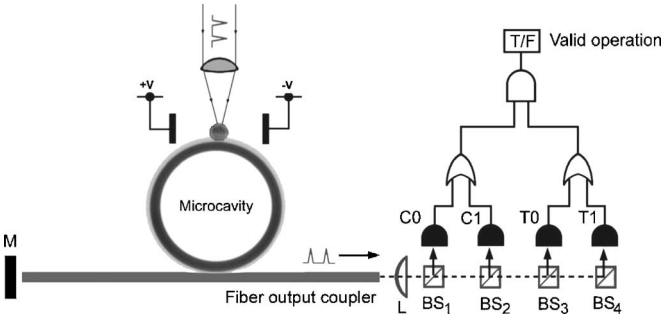

FIG. 5. Proposed readout scheme featuring a fiber taper coupled to the cavity. A mirror (M) reflects photons back toward the detection apparatus. Each mode is detected separately using narrowband frequency-selective beam splitters to send the appropriate photons to single-photon counting detectors. A logic circuit is also indicated, which detects valid gate operations. This can be used to collect meaningful statistics on the gate operation in the presence of gate losses.

play spectral diffusion, which is an indicator of strong polarizability. In particular, the polarizability of CdSe nanocrystals has been thoroughly studied. Stark tuning of the nanocrystal resonance across more than 10 THz was demonstrated.[40] In practice, Stark tuning would need to be restricted to a few gigahertz in order to prevent the qubits having excessively rapid rotating phases. Aside from CdSe, larger nanocrystals would be expected to have a reasonable polarizability due to weaker quantum confinement, while smaller nanocrystals displaying strong quantum confinement should be less polarizable. Therefore it may be possible to choose an appropriate polarizability based on either the quantum dot material or size. In fact a smaller polarizability may be desirable in order to suppress excess noise from spurious or fluctuating fields.

DISCUSSION

The model we have used is a ladder system, which is more appropriate for atomic systems. The biexciton state is a multiparticle state, which is quite unlike a single-atomic system, but more akin to two atoms interacting with a cavity field. This is due to the spin degeneracy of the conduction and valence bands. In general there are two degenerate or nearly degenerate exciton states, both of which are coupled to the same ground and biexciton states. This system thus provides two paths to the same biexciton state and so is extremely phase sensitive. In fact it is possible for destructive quantum interference to suppress population in the biexciton state, which may ultimately allow for a phase gate that is insensitive to biexciton losses. However, this would require a completely different gate operation protocol. Therefore, in order for the proposed model to be applicable, the spin degeneracy of the exciton states needs to be lifted. This can be accomplished using an external magnetic field, but may also be accomplished by crystalline anisotropy, shape anisotropy, or with the addition of a magnetic impurity. Splittings need to be at least an order of magnitude greater than the vacuum Rabi frequency to prevent interference effects from adversely affecting the performance of the gate. For example, if a PbS nanocrystal is used with a vacuum Rabi frequency of 500 MHz, a splitting of around 5 GHz would be required. This magnitude of splitting is readily achieved in GaAs quantum dots with relatively modest magnetic fields.[41] The use of a magnetic field to cause the exciton splitting will result in two exciton states with well-resolved spin angular meomentum. However, this property does not affect the gate operation, as the whispering gallery modes of the microresonator have nondegenerate polarization states, which are the TE and TM modes. Therefore it is not possible for a cavity mode to induce spin-selective transitions. Thus, the cavity mode interactions will obey selection rules applicable to linearly polarized light. This means that the cavity modes can interact with both the exciton and biexciton transitions in a manner suitable for our gate operation.

The photonic CNOT gate based on logical qubits, comprising two distinct field modes, allows detection of errors due to losses in many cases. As the quantum dot is merely acting as a quantum bus, any spontaneous emission losses will translate into field mode losses. Any loss due to spontaneous emission after a CNOT interaction will result in the loss of a quantum, which is in principle detectable. The biexcitonic interaction may in fact be the dominant loss mechanism in this gate. In fact the splitting of the exciton transitions also means there is an unused fourth level in the system. While this level can be detuned sufficiently from the CQED interaction, it nevertheless presents another deexcitation pathway for the biexciton state. This extra pathway results in a return of the quantum dot from the biexciton state to its unexcited state. This presents an additional loss mechanism that results in the total loss of all quanta. The other deexcitation pathway via the state $|X\rangle$ results in the loss of a single quantum. Both losses are detectable and will necessitate rerunning the gate. Therefore, if this loss is not too great, the gate will simply need to be run successively until two photons are detected. For a high-Q cavity the field losses can be made negligible. Within the time frame of the CNOT interaction, the loss in the field modes should be small. However, field mode losses are more likely to occur via the output coupler and so in principle can give rise to undetectable errors in certain cases. There are also certain losses in the field modes that do not effect the gate operation. Only losses in modes that are directly involved in the CNOT interaction can have a possible effect, if the loss occurs before the CNOT interaction. For example, any losses in the control qubit logical $|0\rangle$ state will not affect the outcome of the gate.

The use of two spectrally distinct field modes to comprise a single logical qubit introduces some complications. For instance the phase of the qubit will be rotating at a frequency $\Delta_m/2\pi$, which can be in the gigahertz regime. This provides constraints on the system, as accurate control of the phase is required. Therefore, the mode separation will be constrained by the accuracy of the electronics.

In general, the operation of the photonic CNOT gate based around a conditional phase shift using the biexciton transition in quantum dots seems to yield very high fidelities. Furthermore, the operation is not highly sensitive to biexciton losses. In fact this photonic gate is able to detect all quantum dot losses, as such losses will take the system out of the

computational basis. Therefore, the quantum-dot-based CNOT gate can be operated in the coincidence basis with very high fidelity.

Experimental implementation of the proposed photonic CNOT gate relies primarily on the material properties of the gate's constituents. Recent advances in the fabrication of fused silica microcavities have shown that these devices have the potential to facilitate cavity QED interactions well into the strong cavity-coupling regime.[7,10] The main points that need to be addressed are the fabrication of a microcavity with an appropriate mode structure and also the use of a nanocrystal quantum dot with an appropriate lifetime and with decoherence properties approaching the lifetime limit. A suitable mode structure will probably involve transverse mode engineering. For example, transverse modes in microspheres can have a reasonable mode separation, which should be sufficient for the task.[42]

The first requirement of the nanocrystal is that it must provide an appropriate two-level system. This constraint can already be satisfied by most available nanocrystals as quantum confinement energies are many orders of magnitude greater than predicted coupling energies. This holds true even for the band-edge exciton fine structure. Furthermore, nanocrystal shape modification may provide further ways to modify the spectroscopy in order to provide a suitable two-level system in other nanocrystals.[43] One of the most stringent constraints on the nanocrystal system is the requirement for low decoherence of the excited state. In the solid-state environment, phonons are the main contributors to excited-state decoherence. Optical phonons can easily be removed from the solid-state environment by cooling to temperatures below the optical phonon cutoff energy. However, acoustic phonons are widely dispersive and exist down to zero temperature. Nevertheless, nanocrystal materials are of sufficiently small size that the acoustic phonon band becomes discretized and it becomes possible to cool the system to a temperature below that which can excite the fundamental acoustic phonon mode in the nanocrystal (note that this pertains to colloidal nanocrystals, where a large acoustic mismatch between the nanocrystal and the surrounding matrix can be maintained, allowing discretization of acoustic modes due to finite boundary conditions). A temperature below 20 K is usually sufficient to freeze out all phonons in a nanocrystal. In a phonon-free environment, it is possible to obtain lifetime-limited linewidths.[21,44] Linewidths narrower than k_BT have already been observed in CdSe nanocrystals cooled to below 10 K,[31] and ensemble linewidths close to 1 GHz have been observed.[45] This is very promising for limiting exciton dephasing. Unfortunately, the lowest exciton level is often an optically forbidden transition, or dark state,[46] which causes additional dephasing and even exciton trapping in many different quantum dots. This obstacle does not seem to be present for the IV-VI lead chalcogenide nanocrystals,[47–50] which is very promising.

Therefore we consider the properties of lead sulfide–based nanocrystals, as they possess a number of properties useful for CQED, such as near-infrared emission and very long exciton lifetimes.[19,48,51] If we consider, for example, a PbS nanocrystal with an emission wavelength of 850 nm, an exciton lifetime of 500 ns, and assume a lifetime-limited transition linewidth, direct comparison with the analysis of Buck and Kimble[10] indicates that a coupling frequency of 111 MHz and consequently a ratio of the coupling frequency to the exciton loss rate of $g_X/\gamma_X=300$ can be achieved using a optimal microsphere with a radius $r=7.83$ μm and with a Q of 9.76×10^8.[10] This is well beyond the value of $g_X/\gamma_X=100$ assumed in our simulations.

The lead salts do introduce the additional complication of an eightfold-degenerate ground state, due to the presence of four equivalent band-gap minima. It is predicted that intervalley scattering will split the degenerate ground state,[48] thus providing a suitable isolated exciton level. The lead salts may also offer other advantages due to strong quantum confinement of the charge carriers, such as an inhibition of the Auger scattering rate for certain sizes that provide a minimal density of states for Auger scattering. This could facilitate longer biexciton lifetimes and increased quantum efficiencies. Nevertheless, the presence of extrinsic states, such as surface states is one area that needs to be addressed. There is currently a great deal of research into surface passivation and modification in order to treat these surface states. In fact the most encouraging results recently published show that the phenomenon of blinking can actually be suppressed with the appropriate surface treatment.[52] This has major implications for all sorts of nanocrystal uses, including quantum technologies. Therefore many of the current limitations for using quantum dots in cavity-QED-based technologies are simply technological issues that can be overcome. If there are neither intrinsic nor extrinsic states that can cause additional dephasing in lead-salt-based quantum dots, then it is quite reasonable to suppose that lifetime-limited transition linewidths may be obtained.

Lastly, the technical issues of spectral diffusion and blinking in colloidal nanocrystals are undesirable traits for use in quantum technologies. However, they do not represent an ultimate barrier to future implementation.[34] For instance, under optical excitation, spectral diffusion can be greatly minimized by using low excitation intensities.[31,45] This is also true of blinking.[29] This suggests that nonlinear multiphoton absorption plays a strong part in exacerbating these phenomena. However, while cavity-enhanced single-photon absorption is strongly nonlinear, it does not entail any multiphoton absorption. Therefore we expect that CQED-based nonlinearities should be only marginally affected by these undesirable properties. Nevertheless, any ultimate implementation will require that blinking and spectral diffusion be addressed at a technological level. To this end, certain types of nanoheterostructures have been found to exhibit neither blinking nor spectral diffusion.[30] Most importantly, recent advances in the technology of surface passivation have succeeded in suppressing blinking in commercially available CdSe based nanocrystals.[52] Alternative methods of improved surface passivation could also comprise epitaxial overgrowth of a thick lattice-matched shell. These recent developments in the surface treatment of nanocrystals to improve their optical properties show that there is a clear impetus to close the gap between epitaxially grown SAQD's and colloidal nanocrystals[18,34] that primarily stems from the desire to make robust, optically active but chemically passive nanocrystals for long-term use in numerous technologies. For example,

single colloidal nanocrystals are already being investigated as single-photon sources.[53]

CONCLUSION

We have investigated the use of the Stark-tuning property of a nanocrystal quantum dot in order to control the quantum interaction with a high-Q/V microcavity. A photonic CNOT gate based on the strong cavity coupling between both the excitonic and biexcitonic transitions in a nanocrystal quantum dot and four nondegenerate field modes of a high-Q/V fused silica microcavity was proposed. For this gate, the quantum dot is used only as a quantum bus that transfers and manipulates quantum information contained in the cavity modes. We have attempted to use realistic parameters in our model to obtain a reasonable estimate of what may be obtained experimentally. The manufacture of microcavities with sufficiently low loss and high Q/V ratio can be achieved with existing technology. Once we are well into the strong-coupling regime, we find that initial-state preparation can be accomplished with fidelities greater than 99%.

Recent advances in nanocrystal fabrication have prompted us to consider the use of the biexcitonic transition in nanocrystal quantum dots. A range of biexcitonic loss rates were considered for the simulation, as it has been established that there are additional loss processes for the biexciton state. The entire CNOT gate can operate with over 95% fidelity in the low-loss regime. Furthermore, we have found that the photonic gate is able to produce Bell states with reasonably high fidelity over a wide range of possible biexciton loss rates. This makes the gate potentially useful as a resource for generating photonic Bell pairs.

While the performance of this gate seems promising, it still requires further development in both microcavity fabrication as well as demonstration of appropriate nanocrystal properties, such as high-resolution observation of the exciton and biexciton linewidths as well as the observation of vacuum Rabi splitting or vacuum Rabi oscillations. Further improvements to the gate protocol could involve using quantum interference to relax the contraint on the biexciton loss rate. Nevertheless, the model serves to highlight the possibility of using the dc Stark tunability of a nanocrystal quantum dot as a useful means to control cavity QED interactions for potential quantum technologies, such as highly efficient nonclassical light sources.

[1] E. Knill, R. Laflamme, and G. J. Milburn, Nature (London) **409**, 46 (2001).
[2] J. L. O'Brien, G. J. Pryde, A. G. White, T. C. Ralph, and D. Branning, Nature (London) **426**, 264 (2003).
[3] T. B. Pittman, M. J. Fitch, B. C. Jacobs, and J. D. Franson, Phys. Rev. A **68**, 032316 (2003).
[4] S. Gasparoni, J. W. Pan, P. Walther, T. Rudolph, and A. Zeilinger, Phys. Rev. Lett. **93**, 020504 (2004).
[5] K. Nemoto and W. J. Munro, Phys. Rev. Lett. **93**, 250502 (2004).
[6] D. K. Armani, T. J. Kippenberg, S. M. Spillane, and K. J. Vahala, Nature (London) **421**, 925 (2003).
[7] S. M. Spillane, T. J. Kippenberg, K. J. Vahala, K. W. Goh, E. Wilcut, and H. J. Kimble, Phys. Rev. A **71**, 013817 (2005).
[8] B. S. Song, S. Noda, T. Asano, and Y. Akahane, Nat. Mater. **4**, 207 (2005).
[9] D. W. Vernooy, A. Furusawa, N. P. Georgiades, V. S. Ilchenko, and H. J. Kimble, Phys. Rev. A **57**, R2293 (1998).
[10] J. R. Buck and H. J. Kimble, Phys. Rev. A **67**, 033806 (2003).
[11] J. McKeever, A. Boca, A. D. Boozer, R. Miller, J. R. Buck, A. Kuzmich, and H. J. Kimble, Science **303**, 1992 (2004).
[12] C. Santori, D. Fattal, J. Vuckovic, G. Solomon, and Y. Yamamoto, Nature (London) **419**, 594 (2002).
[13] C. Santori, D. Fattal, J. Vuckovic, G. Solomon, and Y. Yamamoto, Fortschr. Phys. **52**, 1180 (2004).
[14] M. Pelton, C. Santori, J. Vuckovic, B. Y. Zhang, G. S. Solomon, J. Plant, and Y. Yamamoto, Phys. Rev. Lett. **89**, 233602 (2002).
[15] A. Kiraz, M. Atature, and A. Imamoglu, Phys. Rev. A **69**, 032305 (2004).
[16] A. Kiraz, C. Reese, B. Gayral, L. Zhang, W. Schoenfeld, B. Gerardot, P. Petroff, E. Hu, and A. Imamoglu, J. Opt. B: Quantum Semiclassical Opt. **5**, 129 (2003).
[17] X. Q. Li, Y. W. Wu, D. Steel, D. Gammon, T. H. Stievater, D. S. Katzer, D. Park, C. Piermarocchi, and L. J. Sham, Science **301**, 809 (2003).
[18] R. Xie, U. Kolb, J. Li, T. Basche, and A. Mews, J. Am. Chem. Soc. **127**, 7480 (2005).
[19] H. Du, C. Chen, R. Krishnan, T. Krauss, J. Harbold, F. Wise, M. Thomas, and J. Silcox, Nano Lett. **2**, 1321 (2002).
[20] Y. Yin and A. Alivisatos, Nature (London) **437**, 664 (2005).
[21] C. Kammerer, G. Cassabois, C. Voisin, M. Perrin, C. Delalande, Ph. Roussignol, and J. Gerard, Appl. Phys. Lett. **81**, 2737 (2002).
[22] T. Yoshie, A. Scherer, J. Hendrickson, G. Khitrova, H. Gibbs, G. Rupper, C. Ell, O. Shchekin, and D. Deppe, Nature (London) **432**, 200 (2004).
[23] J. Reithmaier, G. Sek, A. Loffler, C. Hofman, S. Kuhn, S. Reitzenstein, L. Keldysh, V. Kulakovskii, T. Reinecke, and A. Forchel, Nature (London) **432**, 197 (2004).
[24] X. D. Fan, M. C. Lonergan, Y. Z. Zhang, and H. L. Wang, Phys. Rev. B **64**, 115310 (2001).
[25] M. V. Artemyev, U. Woggon, R. Wannemacher, H. Jaschinski, and W. Langbein, Nano Lett. **1**, 309 (2001).
[26] N. Le Thomas, U. Woggon, O. Schops, M. V. Artemyev, M. Kazes, and U. Banin, Nano Lett. **6**, 557 (2006).
[27] K. Shimizu, R. Neuhauser, C. Leatherdale, S. Empedocles, K. Woo, and M. Bawendi, Phys. Rev. B **63**, 205316 (2001).
[28] B. Fisher, H.-J. Eisler, N. Stott, and M. Bawendi, J. Phys. Chem. B **108**, 143 (2004).
[29] K. T. Shimizu, R. G. Neuhauser, C. A. Leatherdale, S. A. Empedocles, W. K. Woo, and M. G. Bawendi, Phys. Rev. B **63**, 205316 (2001).
[30] F. Koberling, A. Mews, and T. Basche, Phys. Rev. B **60**, 1921 (1999).
[31] S. A. Empedocles, D. J. Norris, and M. G. Bawendi, Phys. Rev.

Lett. **77**, 3873 (1996).
[32] V. Klimov, A. Mikhailovsky, D. McBranch, C. Leatherdale, and M. Bawendi, Science **287**, 1011 (2000).
[33] A. Rauschenbeutel, G. Nogues, S. Osnaghi, P. Beret, P. Brune, J. Raimond, and S. Haroche, Phys. Rev. Lett. **83**, 5166 (1999).
[34] B. Fisher, J. M. Caruge, D. Zehnder, and M. Bawendi, Phys. Rev. Lett. **94**, 087403 (2005).
[35] J. M. Caruge, Y. T. Chan, V. Sundar, H. J. Eisler, and M. G. Bawendi, Phys. Rev. B **70**, 085316 (2004).
[36] R. Ellingson, M. Beard, J. Johnson, P. Yu, O. Micic, A. Nozik, A. Shabaev, and A. Efros, Nano Lett. **5**, 865 (2005).
[37] P. M. Radmore and P. L. Knight, J. Phys. B **15**, 561 (1982).
[38] E. H. Huntington and T. C. Ralph, J. Opt. B: Quantum Semiclassical Opt. **4**, 123 (2002).
[39] E. H. Huntington and T. C. Ralph, Phys. Rev. A **69**, 042318 (2004).
[40] S. A. Empedocles and M. G. Bawendi, Science **278**, 2114 (1997).
[41] G. Chen, N. Bonadeo, D. Steel, D. Gammon, D. Katzer, D. Park, and L. Sham, Science **289**, 1906 (2000).
[42] M. Cai, O. Painter, and K. Vahala, Phys. Rev. Lett. **85**, 74 (2000).
[43] X. G. Peng, L. Manna, W. D. Yang, J. Wickham, E. Scher, A. Kadavanich, and A. P. Alivisatos, Nature (London) **404**, 59 (2000); J. T. Hu, L. S. Li, W. D. Yang, L. Manna, L. W. Wang, and A. P. Alivisatos, Science **292**, 2060 (2001); J. T. Hu, L. W. Wang, L. S. Li, W. D. Yang, and A. P. Alivisatos, J. Phys. Chem. B **106**, 2447 (2002).
[44] N. Bonadeo, J. Erland, D. Gammon, D. Park, D. Katzer, and D. Steel, Science **282**, 1473 (1998).
[45] P. Palinginis, S. Tavenner, M. Lonergan, and H. Wang, Phys. Rev. B **67**, 201307(R) (2003).
[46] Al. Efros, M. Rosen, M. Kuno, M. Nirmal, D. Norris, and M. Bawendi, Phys. Rev. B **54**, 4843 (1996).
[47] I. Kang and F. W. Wise, J. Opt. Soc. Am. B **14**, 1632 (1997).
[48] G. Allan and C. Delerue, Phys. Rev. B **70**, 245321 (2004).
[49] A. Andreev and A. Lipovskii, Phys. Rev. B **59**, 15402 (1999).
[50] G. Tudury, L. Marquezini, L. Ferreira, L. Barbosa, and C. Cesar, Phys. Rev. B **62**, 7357 (2000).
[51] B. Wehrenberg, C. Wang, and P. Guyot-Sionnest, J. Phys. Chem. B **106**, 10634 (2002).
[52] S. Hohng and T. Ha, J. Am. Chem. Soc. **126**, 1324 (2004).
[53] X. Brokmann, E. Giacobino, M. Dahan, and J. Hermier, Appl. Phys. Lett. **85**, 712 (2004).